



Research Article

Comprehensive Analysis of Density of States (DOS), UV-Visible, NMR Spectroscopy, and Molecular Electrostatic Potential (MEP) of RU-486 and its Derivatives (Ph, KOH, NO₂, OH) in Relation to Their Effects on Breast Cancer †

Mehmet Hanifi KEBİROĞLU*^{1,2}, Fermin AK¹

¹Malatya Turgut Özal University, Darende Bekir Ilıcak Vocational School, Department of Medical Services and Techniques/Opticianry Pr., 44700, Malatya, Türkiye

²Firat University, Faculty of Science, Department of Physics, 23119, Elazığ, Türkiye

*Corresponding author e-mail: hanifi.kebiroglu@ozal.edu.tr

Abstract: In this study, a comprehensive analysis was conducted on RU-486 (Mifepristone) and its derivatives (Ph, KOH, NO₂, OH), focusing on their potential effectiveness against breast cancer. The analysis included Density of States (DOS) optimization, UV-Visible spectroscopy, Nuclear Magnetic Resonance (NMR) spectroscopy, and Molecular Electrostatic Potential (MEP) mapping. The electronic structures and stabilities of these molecules were examined through DOS, revealing how different functional groups influence their electronic properties. UV-Visible spectroscopy identified shifts in absorption maxima, which correspond to changes in electronic transitions due to functionalization. NMR spectroscopy provided insights into the chemical environments of specific nuclei, offering detailed information on molecular geometry and electronic distribution. MEP analysis mapped the electrostatic potential across the molecular surfaces, pinpointing regions of electrophilic and nucleophilic reactivity. Collectively, these analyses have enhanced the understanding of the electronic properties, reactivity, and potential pharmaceutical applications of RU-486 and its derivatives in breast cancer treatment.

Keywords: DOS, MEP, NMR, Ru-486, UV-Vis

RU-486 ve Türevlerinin (Ph, KOH, NO₂, OH) Yoğunluk Durumu (DOS), UV-Görünür, NMR Spektroskopisi ve Moleküler Elektrostatik Potansiyel (MEP) Üzerine Kapsamlı Analizi ve Meme Kanseri Üzerindeki Etkileri ile İlişkisi

Öz: Bu çalışmada, RU-486 (Mifepriston) ve türevleri (Ph, KOH, NO₂, OH) üzerine meme kanserine karşı potansiyel etkinliklerine odaklanılarak kapsamlı bir analiz gerçekleştirilmiştir. Analiz, Yoğunluk Durumu (DOS) optimizasyonu, UV-Görünür spektroskopisi, Nükleer Manyetik Rezonans (NMR) spektroskopisi ve Moleküler Elektrostatik Potansiyel (MEP) haritalandırmasını içermektedir. DOS aracılığıyla bu moleküllerin elektronik yapıları ve kararlılıkları incelenmiş ve farklı fonksiyonel grupların elektronik özellikler üzerindeki etkileri ortaya konmuştur. UV-Görünür spektroskopisi, fonksiyonelleştirme nedeniyle elektronik geçişlerdeki değişimlere karşılık gelen absorpsiyon maksimumlarında kaymalar belirlemiştir. NMR spektroskopisi, belirli çekirdeklerin kimyasal ortamları hakkında detaylı bilgi sağlayarak moleküler geometrinin ve elektronik dağılımın anlaşılmasına katkıda bulunmuştur. MEP analizi, moleküler yüzeylerdeki elektrostatik potansiyeli haritalandırarak elektofilik ve nükleofilik reaktivite bölgelerini belirlemiştir. Bu analizler bir araya getirildiğinde, RU-486 ve türevlerinin elektronik özellikleri, reaktiviteleri ve meme kanseri tedavisindeki potansiyel farmasötik uygulamaları hakkındaki çalışmalar artırmıştır.

Anahtar Kelimeler: DOS, MEP, NMR, Ru-486, UV-Vis

† This article was derived from the doctoral thesis of Mehmet Hanifi KEBİROĞLU and supported by the 100/2000 scholarship program from the Council of Higher Education (YÖK)

Received: 02.11.2024

Accepted: 12.03.2025

How to cite: Kebiroğlu, M. H., & Ak, F. (2025). Comprehensive analysis of density of states (DOS), UV-visible, NMR spectroscopy, and molecular electrostatic potential (MEP) of RU-486 and its derivatives (Ph, KOH, NO₂, OH) in relation to their effects on breast cancer. *Yuzuncu Yil University Journal of the Institute of Natural and Applied Sciences*, 30(1), 46-60. <https://doi.org/10.53433/yyufbed.1578071>

1. Introduction

Breast cancer continues to be a major global health problem, with a significant proportion of cases attributed to reproductive factors, particularly those related to hormonal exposure throughout a woman's life (Obeagu & Obeagu, 2024). Progesterone, a key hormone in female reproductive physiology, is recognized for its role as a major mitogen in breast tissue, promoting the proliferation of breast epithelial cells during the luteal phase of the menstrual cycle (Bartkowiak-Wieczorek et al., 2024). Given the critical role of progesterone in breast tissue dynamics and tumorigenesis, there is increasing interest in the potential of progesterone receptor antagonists as a preventive strategy against breast cancer (Utjés et al., 2024). Mifepristone, a well-known PR modulator, has shown promising results in preclinical and clinical studies due to its ability to counteract the mitogenic effects of progesterone in the breast (Ciebiera et al., 2024). Despite these encouraging findings, the molecular mechanisms underlying the protective effects of mifepristone on normal breast tissue remain poorly understood (Elia et al., 2024). This study contributes to a deeper understanding of the molecular changes induced by progesterone antagonism and highlights the potential of mifepristone as a chemo preventive agent against breast cancer (Iftikhar et al., 2024). It represents the first in vivo examination of the breast transcriptome following mifepristone treatment and provides valuable insight into the early molecular events that may underlie its protective effects (Narwal et al., 2024). Breast cancer is one of the most common malignant tumors worldwide, and metastasis is a leading cause of death among patients (Mustafa et al., 2024). The tumor microenvironment (TME) plays a key role in breast cancer progression, particularly in drug resistance and distant metastasis (Kundu et al., 2024). Within the TME, cancer-associated fibroblasts (CAFs) are activated by tumor cells, leading to the secretion of pro-tumor factors and the production of extracellular matrix (ECM) components that impede drug penetration and facilitate epithelial-mesenchymal transition (EMT) (Zheng & Hao, 2024). In addition, glucocorticoids (GCs) may interact with glucocorticoid receptors (GRs) on breast cancer cells, contributing to immunosuppression and promoting metastasis (He et al., 2024). Recent strategies have focused on combining TME-modulating agents with chemotherapeutic approaches to enhance antitumor efficacy (Zhang et al., 2024a). Natural compounds such as Berberine (Ber) have been shown to inhibit CAF activation and ECM deposition while blocking the TGF- β /Smad2/3-mediated signaling pathway involved in tumor metastasis (Wu et al., 2024). Mifepristone (Ru486), known for its abortifacient properties, has shown antitumor activity by antagonizing GRs and inhibiting GC-GR-mediated metastasis. To overcome the limitations of traditional drug formulations, such as low bioavailability and systemic toxicity, the development of nanosized drug delivery systems has attracted significant attention (Lv et al., 2024). These systems, including liposomes and micelles, can co-deliver multiple drugs with different antitumor mechanisms, thereby enhancing targeted delivery and therapeutic efficacy (Xue et al., 2024). Nanosized carriers modified with hyaluronic acid (HA) show promise in improving drug penetration and targeting tumor cells via CD44 receptor-mediated endocytosis (Chen et al., 2024). The efficacy of these formulations was evaluated in vitro using the "MCF-7/MRC-5" dual-cell model and in vivo using the orthotopic 4T1 cell mouse model (Wu et al., 2024). The results showed that D-HMs and B&R-HLs effectively penetrated tumor tissues, inhibited CAF activation, reduced ECM deposition, and decreased tumor angiogenesis, ultimately leading to significant inhibition of breast cancer metastasis (Sayed et al., 2024). Density Functional Theory (DFT) calculations were performed to analyze the theoretical absorbance spectra, HOMO-LUMO orbitals, density of states (DOS) spectra, and various molecular properties. RU-486 (Mifepristone) and its derivatives are considered promising agents in breast cancer treatment by targeting progesterone and glucocorticoid receptors (Naqvi et al., 2025). Due to their potential to inhibit tumor growth and slow down metastatic processes, research on these compounds for breast cancer prevention and treatment has been steadily increasing (Xiong et al., 2025). Additionally, incorporating nanotechnological drug delivery systems can enhance the efficacy of RU-486, providing a more specific and potent antitumor effect (Mohammad-Jafari et al., 2024).

2. Material and Methods

2.1. Molecular structure Optimization

The molecular structures of RU-486 (Mifepristone) and its derivatives (Ph, KOH, NO₂, OH) were optimized using Density Functional Theory (DFT), a quantum mechanical modeling method widely used in computational chemistry to predict molecular geometries and electronic properties with high accuracy. The optimization was carried out using the B3LYP functional combined with the 6-311++G(d,p) basis set, which ensures precise treatment of electron correlation effects and provides reliable structural parameters (Kumar et al., 2024). Once the optimization process was completed, frequency calculations were performed to confirm that each geometry corresponded to a true local minimum on the potential energy surface. This step is crucial because imaginary frequencies would indicate a transition state rather than a stable molecule. The absence of imaginary frequencies verified that the structures obtained were stable conformations (Tegegn et al., 2024). The optimized molecular geometries obtained from this study serve as a foundation for further investigations, including electronic structure analysis (DOS), spectroscopic simulations (UV-Vis, NMR), and Molecular Electrostatic Potential (MEP) mapping, providing valuable insights into the potential applications of RU-486 derivatives.

The Density of States (DOS) analysis was performed to investigate the effects of different functional groups (Ph, KOH, NO₂, OH) on the electronic structures of RU-486 and its derivatives (Middleton et al., 2024). DOS analysis provides critical insight into the distribution of electronic energy levels and how functionalization influences molecular electronic properties (Zaki et al., 2025).

Time-Dependent DFT (TD-DFT) was employed to simulate the UV-Visible absorption spectra of RU-486 and its derivatives (Ghazy et al., 2024). These calculations were conducted in the gas phase at the same B3LYP/6-311++G(d,p) theoretical level, with absorption maxima (λ_{max}) analyzed to observe the changes in electronic transitions resulting from functionalization of the parent molecule (Aloumko et al., 2024). The NMR chemical shifts of RU-486 and its derivatives were calculated using the Gauge-Independent Atomic Orbital (GIAO) method at the B3LYP/6-311++G(d,p) level (Liu et al., 2024). Proton (¹H) and carbon (¹³C) NMR spectra were generated, and the chemical environments of specific nuclei were analyzed (Zhang et al., 2024b). The chemical shifts were referenced against Tetramethylsilane (TMS) as an internal standard, providing detailed information about molecular geometry and electronic distribution (Seqqat et al., 2025).

Molecular Electrostatic Potential (MEP) maps were generated to visualize the electrostatic potential across the molecular surfaces of RU-486 and its derivatives (Chatterjee et al., 2024). MEP calculations were performed using the optimized geometries from the DFT calculations at the B3LYP/6-311++G(d,p) level. The MEP maps were analyzed to identify regions of electrophilic and nucleophilic reactivity, which are critical for understanding the interactions of these molecules with biological targets (Şahin, 2023).

The computational data obtained from these analyses were used to compare the electronic properties, chemical reactivity, and potential biological activity of RU-486 and its derivatives. The DOS, UV-Visible spectra, NMR chemical shifts, and MEP maps were collectively examined to draw conclusions regarding the influence of different functional groups on the molecular properties and their effectiveness in breast cancer treatment (Manakkadan et al., 2024).

3. Results

3.1. Geometry optimization

Geometry optimization is a critical process in molecular modeling, aimed at determining the most stable, low-energy configuration of a molecule (Pracht et al., 2024). This process begins with an initial geometry setup, followed by energy minimization, typically performed using advanced quantum chemistry software such as Gaussian 09 (Cao et al., 2024). In this study, the geometry of the RU-486 molecule was optimized in both its pure form and when doped with various functional groups (Ph, KOH, NO₂, OH). These modifications led to distinct molecular conformations, each representing the molecule's lowest energy state (Chaudhuri et al., 2024). Understanding these optimized structures is

essential for analyzing molecular properties, investigating chemical reaction mechanisms, and designing new pharmaceutical compounds. The optimization results, calculated using both DFT and HF approaches, are presented in Figure 1 and Table 1 (Yılmaz & Kebiroğlu, 2024).

Table 1. Structural and electronic changes in RU-486 molecule due to various dopants (Ph, KOH, NO₂, OH)

| Doped Molecule | Dopant Description | Structural Changes | Electronic Changes |
|------------------------------|--|---|--|
| Ph Doped RU-486 | Phenyl group (Ph) is a benzene ring attached to RU-486. | Introduces a significant structural component, altering the molecular conformation. | Affects overall geometry and electronic properties of the RU-486 molecule. |
| KOH Doped RU-486 | Potassium hydroxide (KOH), consisting of potassium (purple atom) and hydroxyl (OH) groups. | Causes significant changes in the molecular structure due to interaction with potassium and hydroxyl. | Alters the spatial arrangement and electronic distribution within the RU-486 molecule. |
| NO ₂ Doped RU-486 | Nitro group (NO ₂), consisting of one nitrogen (blue atom) and two oxygen atoms (red atoms). | Significantly influences the molecular structure, integrating into the RU-486 framework. | Alters conformation and electronic properties of the molecule. |
| OH Doped RU-486 | Hydroxyl group (OH), consisting of one oxygen (red atom) and one hydrogen atom. | Affects the molecular structure and interactions, altering the overall molecular conformation. | Influences the electronic distribution within the molecule. |

3.2. Molecular electrostatic potential (MEP) maps

Electrostatic potential maps (MEP) are essential for analyzing the distribution of electronegativity and partial charges within molecules, highlighting regions prone to electrophilic (red) and nucleophilic (blue) attacks (Rajimon et al., 2024). This color-coded visualization helps in understanding molecular interactions, such as bonding with biological molecules, and identifying reactive sites. For the RU-486 molecule and its derivatives, MEP analysis indicates a tendency toward nucleophilic behavior, with green areas representing moderate electron density and potential electrophilic regions (Irfan et al., 2024). These findings, shown in Figure 2 and Table 2, provide valuable insights into the chemical behavior and interaction potential of these molecules. Additionally, the separation between the green and red lines represents the energy difference between the HOMO and LUMO levels for all elements (Çankaya et al., 2024).

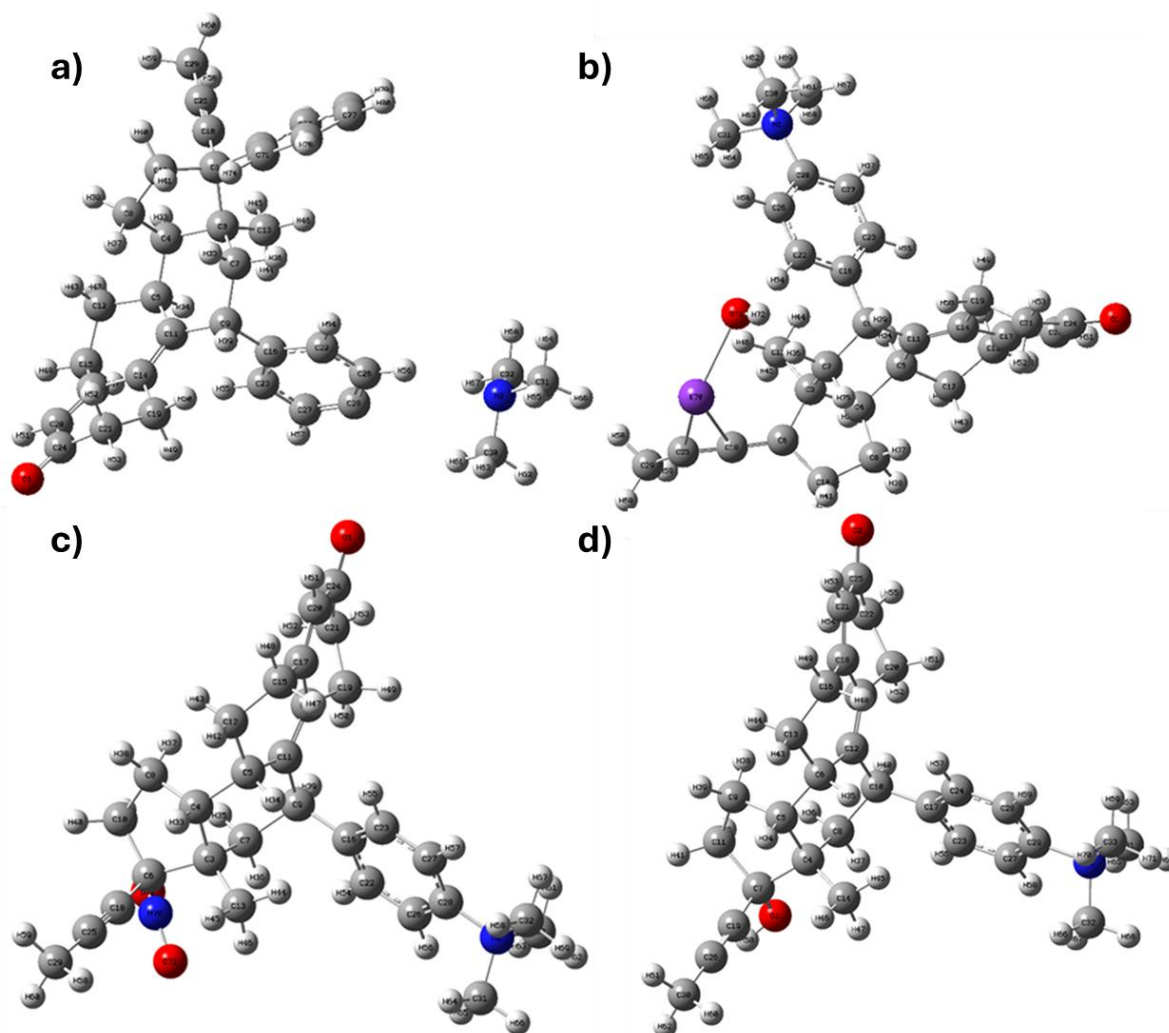


Figure 1. Optimized structure of RU-486 molecule a) Ph b) KOH c) NO₂ d) OH doped.

Table 2. Molecular electrostatic potential (MEP) maps and electron density distributions of RU-486 doped with various functional groups (Ph, KOH, NO₂, OH)

| Molecule | MEP Map Description | Electron Density Distribution | Chemical Implications |
|------------------------|--|---|--|
| RU-486-Ph | RU-486 doped with a phenyl group (Ph). | Red regions around the aromatic ring indicate high electron density (electron-rich areas). | Likely sites for electrophilic attacks due to the electron-rich nature of the aromatic ring. |
| RU-486-KOH | RU-486 doped with a potassium hydroxide (KOH) group. | Potassium is shown in blue (electron-poor), oxygen in red (electron-rich), with green/yellow indicating moderate density. | KOH group creates distinct areas for potential chemical interactions, influencing overall electron distribution. |
| RU-486-NO ₂ | RU-486 doped with a nitro group (NO ₂). | Red regions around oxygen atoms of the nitro group indicate high electron density. | Potential sites for nucleophilic attacks; nitro group significantly alters overall reactivity and interactions. |
| RU-486-OH | RU-486 doped with a hydroxyl group (OH). | Red region around the oxygen atom shows high electron density; blue areas suggest lower density regions. | Hydroxyl group affects electrophilic and nucleophilic regions, altering the molecule's chemical reactivity. |

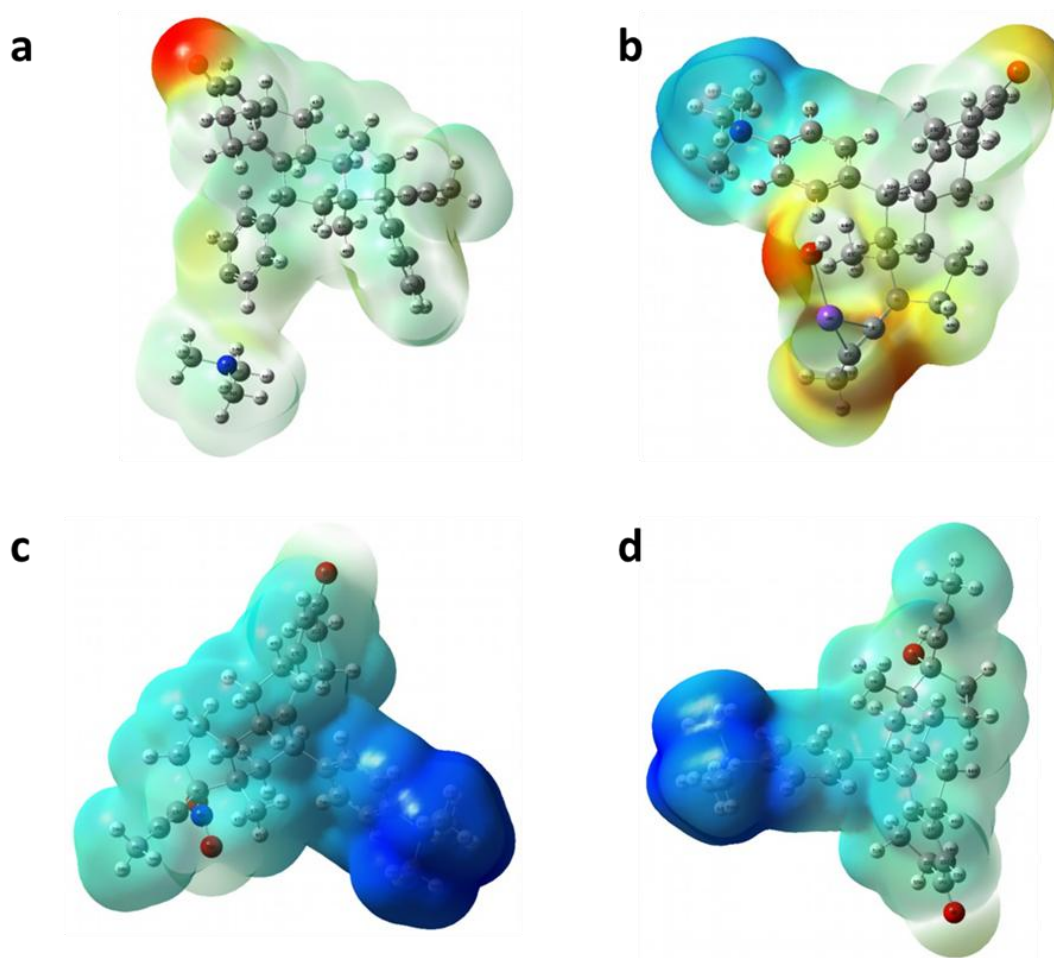


Figure 2. MEP maps of a) RU-486-Ph b) RU-486-KOH, c) RU-486-NO₂, d) RU-486-OH molecules.

3.3. Vibrational spectroscopic analysis spectrum

If the dipole moment of a molecule changes during vibration, the vibrational mode becomes infrared-active, meaning it can absorb infrared light (Mello et al., 2024). Symmetric vibrations, however, are rarely observed in the infrared spectrum, particularly in molecules with a center of symmetry where these vibrations are inactive (Esselman et al., 2024). Asymmetric vibrations are detectable for all molecules, allowing the investigation of various chemical groups, including amino acids and water molecules, which are challenging to detect with conventional spectroscopy (Araújo et al., 2024). In this study, the vibrational spectra of RU-486 and its derivatives were analyzed using the DFT/B3LYP method and the 6-31G basis set. The resulting IR spectra, covering the 3500-0 cm⁻¹ range, display absorption peaks that reflect the vibrational frequencies, which are influenced by bond strength and the mass of the bonded atoms. The similarity in spectra and vibrational frequencies across complexes indicates similar structural properties.

Table 3. Summary of peak intensities and frequencies in Figure 3a to Figure 3d with associated low-level transmittance changes

| Figure | Peak Number with Highest Intensity | Wavenumber (cm ⁻¹) | Other Transmittance Numbers with Low-Level Changes |
|-----------|------------------------------------|--------------------------------|--|
| Figure 3a | 8 | 3108 | 67, 26, 36, 15, 14, 27, 54, 64, 80, 82, 88 |
| Figure 3b | 0.1 | 3073 | 8, 26, 25, 23, 20, 10, 30, 50, 51, 15, 16 |
| Figure 3c | 9 | 3100 | 69, 25, 20, 16, 26, 20, 47, 64, 79, 81 |
| Figure 3d | 6 | 3091 | 81, 30, 42, 19, 34, 17, 57, 70, 38 |

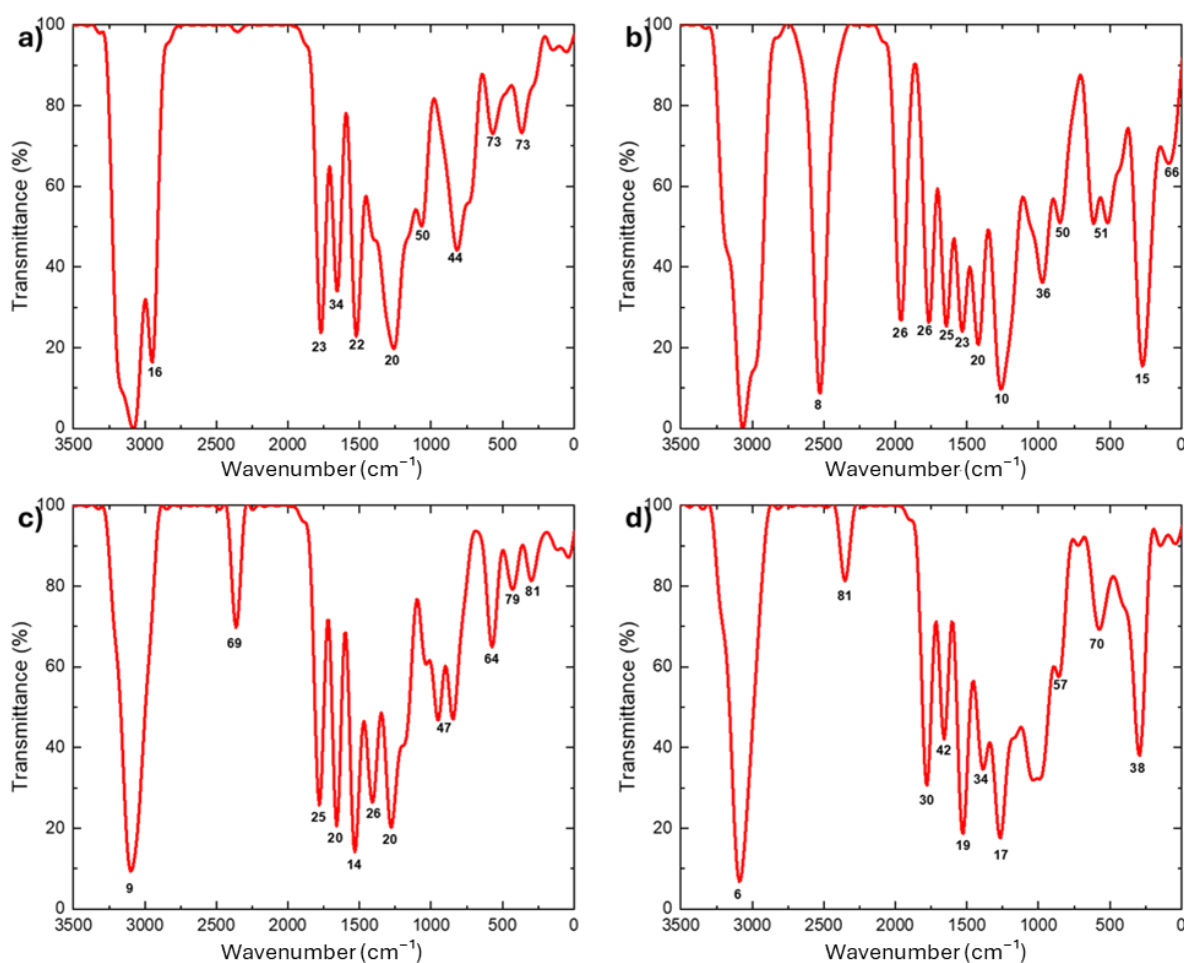


Figure 3. FT-IR spectrum of a) Ru-486-Ph b) Ru-486-KOH, c) Ru-486-NO₂, d) Ru-486-OH molecules.

3.4. Nuclear magnetic resonance spectroscopy

3.4.1. ¹³C NMR spectrum

The ¹³C NMR (Nuclear Magnetic Resonance) spectrum is a form of nuclear magnetic resonance spectroscopy used to identify different carbon environments within a molecule, helping to determine the structure of organic compounds (Günther, 2013). In the ¹³C NMR spectrum of RU-486 in Figure 4, Mifepristone exhibits a complex structure, with details of RU-486 and its derivatives in Table 4.

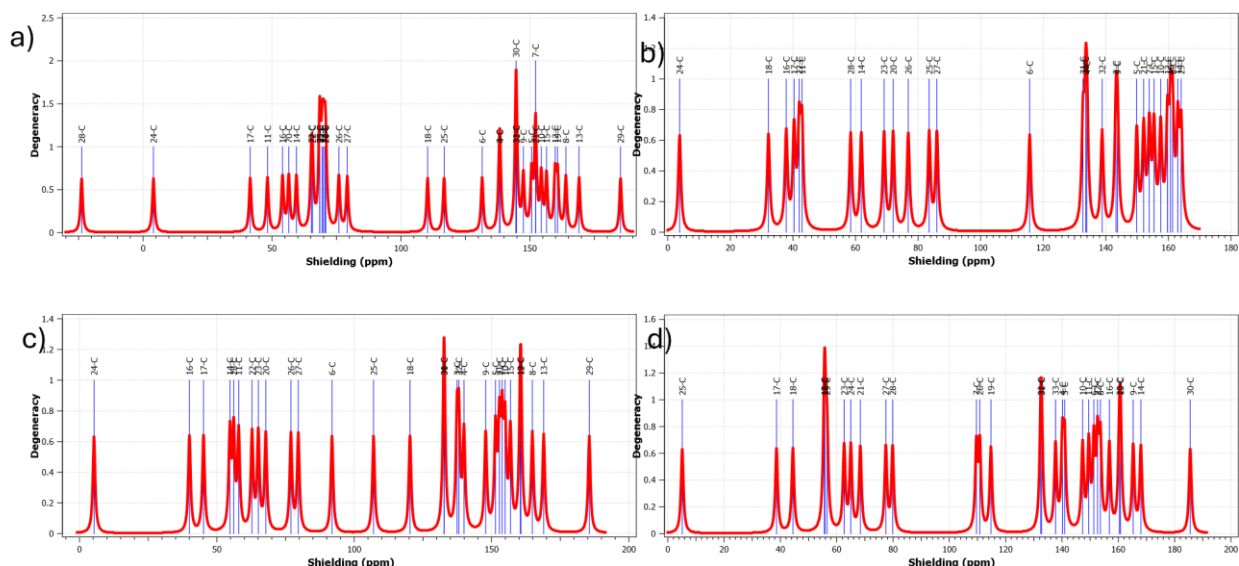


Figure 4. ¹³C NMR spectrum of a) Ru-486-Ph b) Ru-486-KOH, c) Ru-486-NO₂, d) Ru-486-OH molecules.

Table 4. ¹³C NMR spectra for Ru-486 and its derivatives

| Compound | Region (ppm) | Peak Assignment |
|------------------------|--------------|---|
| Ru-486-Ph | 0-50 | Peaks in this region likely correspond to alkyl carbons in the structure, such as methylene (CH ₂) and methyl (CH ₃) groups. |
| | 50-100 | Peaks in this region could correspond to carbons attached to electronegative atoms, possibly indicating carbons connected to oxygen or nitrogen atoms. |
| | 100-150 | This region includes aromatic and olefinic carbons. Given that Ru-486-Ph includes a phenyl (Ph) group, multiple peaks should appear in this region representing the aromatic carbons. |
| | 150-220 | This region typically corresponds to carbonyl carbons (C=O). Ketone or other carbonyl groups in Ru-486 and its derivatives would be indicated by peaks in this region. |
| Ru-486-KOH | 0-50 | Alkyl carbons |
| | 50-100 | Carbons attached to oxygen or other electronegative atoms |
| | 150-220 | Carbonyl carbons (C=O) |
| Ru-486-NO ₂ | 0-50 | Alkyl carbons |
| | 50-100 | Carbons attached to nitro group (NO ₂ , de-shielding, downfield shift) |
| | 150-220 | Carbonyl carbons (C=O) |
| Ru-486-OH | 0-50 | Alkyl carbons |
| | 50-100 | Carbons attached to oxygen atoms (hydroxyl groups, de-shielding) |
| | 150-220 | Carbonyl carbons (C=O) |

3.4.2. ¹H NMR spectrum

The ¹H NMR (Nuclear Magnetic Resonance) spectrum is a powerful technique for determining the structure of organic compounds by identifying the different proton environments within a molecule (Chalbot & Kavouras, 2014). Figure 5 presents the ¹H NMR spectra for a) Ru-486-Ph, b) Ru-486-KOH, c) Ru-486-NO₂, and d) Ru-486-OH molecules. Table 5 provides the detailed ¹H NMR spectra for Ru-486 and its derivatives.

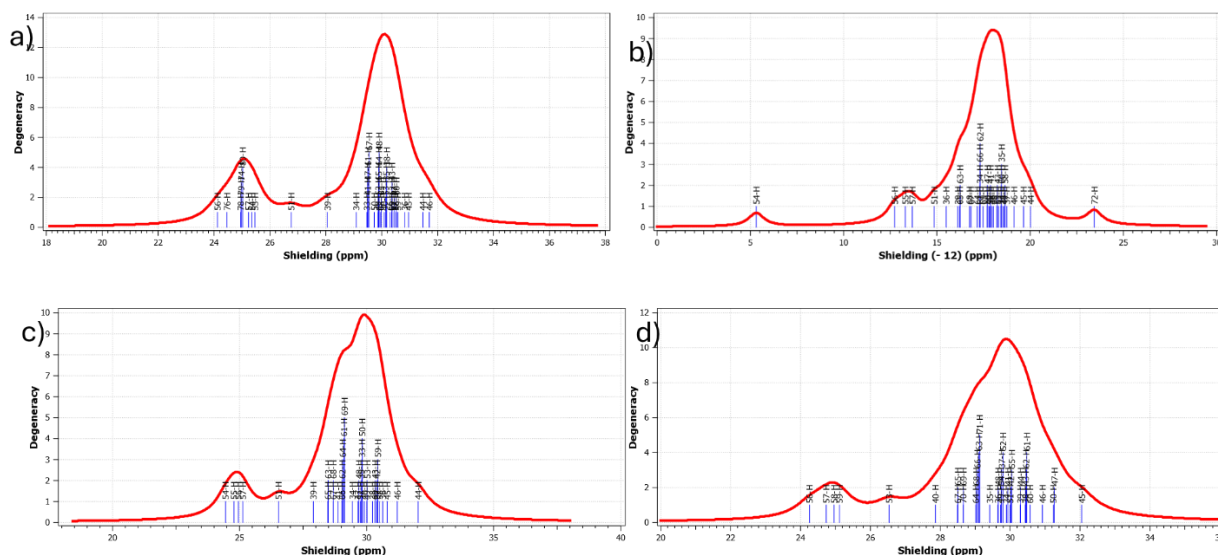


Figure 5. ¹H NMR spectrum of a) Ru-486-Ph b) Ru-486-KOH, c) Ru-486-NO₂, d) Ru-486-OH molecules.

Table 5. ¹H NMR spectra for Ru-486 and its derivatives

| Compound | Region (ppm) | Peak Assignment |
|------------------------|--------------|---|
| Ru-486-Ph | 0-3 | Likely corresponds to alkyl protons, including methylene (CH ₂) and methyl (CH ₃) groups. Peaks around 1.0-2.5 ppm likely represent the protons of the methyl groups. |
| | 3-5 | Protons attached to sp ³ hybridized carbons adjacent to electronegative atoms such as oxygen or nitrogen. |
| | 5-7 | This region usually corresponds to olefinic protons (protons on sp ² carbons in alkenes). Significant activity around this region indicates olefinic protons. |
| | 6-9 | Aromatic protons typically appear in this region. Multiple peaks indicate the aromatic protons in the structure of Ru-486-Ph. |
| | 9-12 | Protons attached to carbonyl groups (aldehydes) or carboxylic acids. No significant peaks suggest a lack of aldehyde or carboxylic acid protons. |
| Ru-486-KOH | 0-3 | Alkyl protons (CH ₂ and CH ₃ groups), peaks around 1.0-2.5 ppm |
| | 3-5 | Protons attached to sp ³ carbons adjacent to electronegative atoms (O) |
| | 5-7 | Olefinic protons (sp ² carbons in alkenes) |
| | 6-9 | Aromatic protons |
| | 9-12 | No significant peaks (absence of aldehyde or carboxylic acid protons) |
| Ru-486-NO ₂ | 0-3 | Alkyl protons (CH ₂ and CH ₃ groups), peaks around 1.0-2.5 ppm |
| | 3-5 | Protons attached to sp ³ carbons adjacent to electronegative atoms (NO ₂) |
| | 5-7 | Olefinic protons (sp ² carbons in alkenes) |
| | 6-9 | Aromatic protons |
| | 9-12 | No significant peaks (absence of aldehyde or carboxylic acid protons) |
| Ru-486-OH | 0-3 | Alkyl protons (CH ₂ and CH ₃ groups), peaks around 1.0-2.5 ppm |
| | 3-5 | Protons attached to sp ³ carbons adjacent to electronegative atoms (OH) |
| | 5-7 | Olefinic protons (sp ² carbons in alkenes) |
| | 6-9 | Aromatic protons |
| | 9-12 | No significant peaks (absence of aldehyde or carboxylic acid protons) |

3.4.3. UV-Visible analysis

UV and UV-visible spectroscopy have played a crucial role in the discovery of atomic and molecular structures by chemists (Rahuman et al., 2020). These optical-based methods have further advanced the study of optical and electronic properties of nanoscale particles. The principle of UV-Visible analysis is based on the absorption of photons by molecules, where interaction with photons in the UV or visible spectrum causes electrons to transition from lower to higher energy levels (Keçiroğlu

& Yılmaz, 2023). Figure 6 presents the UV-visible absorption spectra for a) RU-486-Ph, b) RU-486-KOH, c) RU-486-NO₂, and d) RU-486-OH molecules, while Table 6 details the absorbance spectra and peaks for RU-486 and its derivatives.

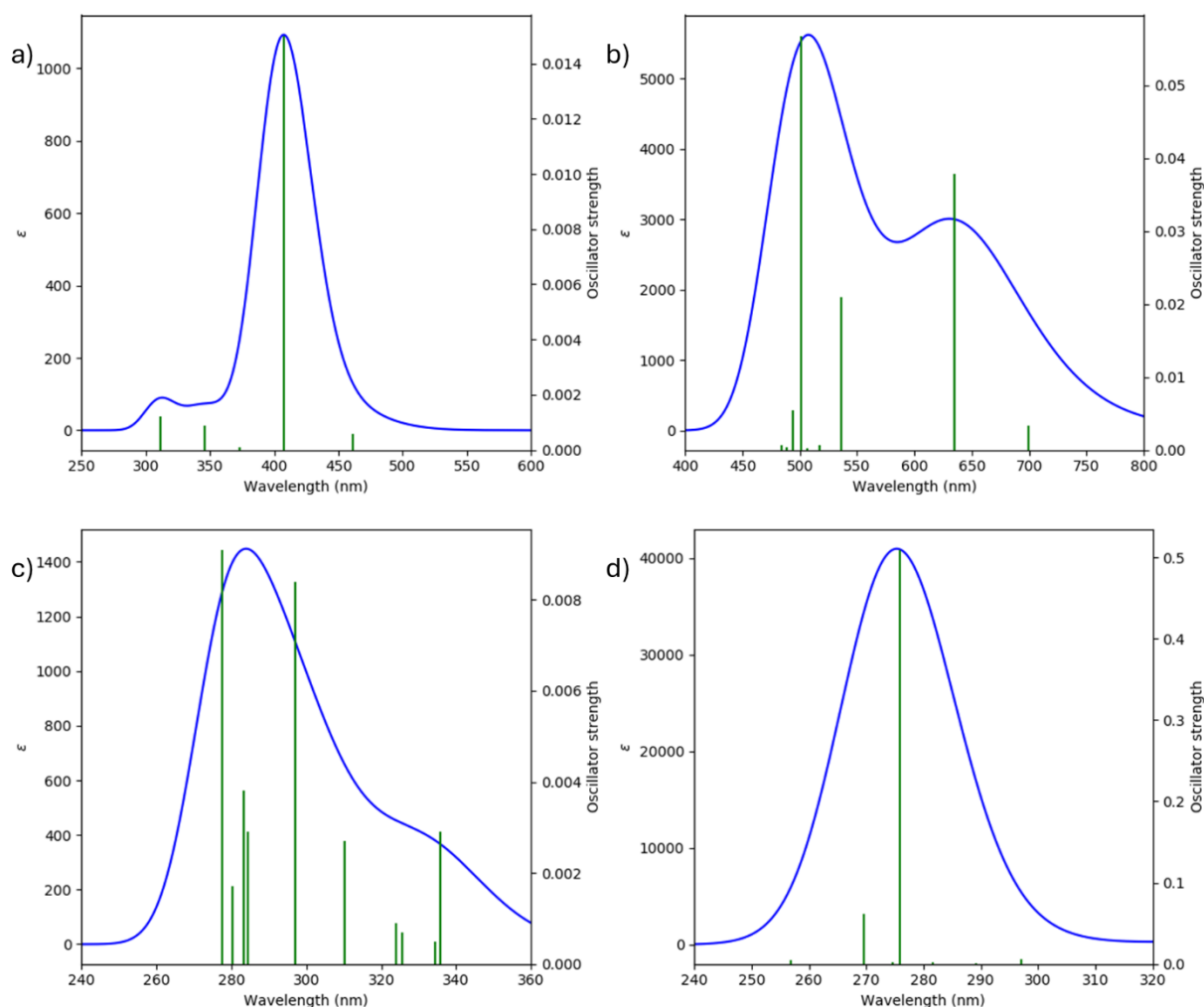


Figure 6. UV-visible absorption of a) Ru-486-Ph, b) Ru-486-KOH, c) Ru-486-NO₂, d) Ru-486-OH molecules.

Table 6. Absorbance spectra and peaks for Ru-486 and its derivatives

| Figure | Compound | Peak Wavelength (nm) | Energy (eV) | Description |
|--------|------------------------|----------------------|-------------|---|
| 6a | RU-486-Ph | 408 | 4.276 | The peak indicates the color of the Ph-doped RU-486 molecule. |
| 6b | RU-486-KOH | 524 | 1.137 | The peak indicates the color of the KOH-doped RU-486 molecule. |
| 6c | RU-486-NO ₂ | 287 | 4.086 | The peak indicates the color of the NO ₂ -doped RU-486 molecule. |
| 6d | RU-486-OH | 287 | 4.094 | The peak indicates the color of the OH-doped RU-486 molecule. |

3.4.4. Density of states (DOS)

The density of states (DOS) is a crucial physical quantity that represents the number of electronic states available at specific energy levels within a material (Kebiroğlu & Ak, 2023). DOS plays a vital role in fields like solid-state physics and materials science, providing insights into the electronic properties of materials (Aghdasi et al., 2024). The Energy (eV) Axis (X-axis) represents these energy

levels in electron volts, typically ranging from approximately -20 eV to +10 eV. In Figure 7 and Table 7, the DOS for a) RU-486-Ph, b) RU-486-KOH, c) RU-486-NO₂, and d) RU-486-OH molecules is illustrated.

Table 7. Overview of density of states (DOS) parameters and energy levels for Ru-486 and its derivatives

| Feature | Description |
|-------------------------------|--|
| DOS Axis (Y-axis) | Represents the density of states, indicating the number of electronic states available at each energy level. |
| Color-Coded Spectra | <ul style="list-style-type: none"> - Alpha DOS spectrum (blue): Density of states for alpha spin electrons. - Beta DOS spectrum (green): Density of states for beta spin electrons. - Total DOS spectrum (red): Combined density of states for both alpha and beta spin electrons, scaled by 0.5 for better visualization. |
| Occupied and Virtual Orbitals | <ul style="list-style-type: none"> - Alpha Occupied Orbitals (cyan): Energy levels where alpha spin electrons are likely to be found in occupied states. - Alpha Virtual Orbitals (magenta): Energy levels where alpha spin electrons are likely to be found in virtual (unoccupied) states. - Beta Occupied Orbitals (yellow): Energy levels where beta spin electrons are likely to be found in occupied states. - Beta Virtual Orbitals (black): Energy levels where beta spin electrons are likely to be found in virtual (unoccupied) states. |

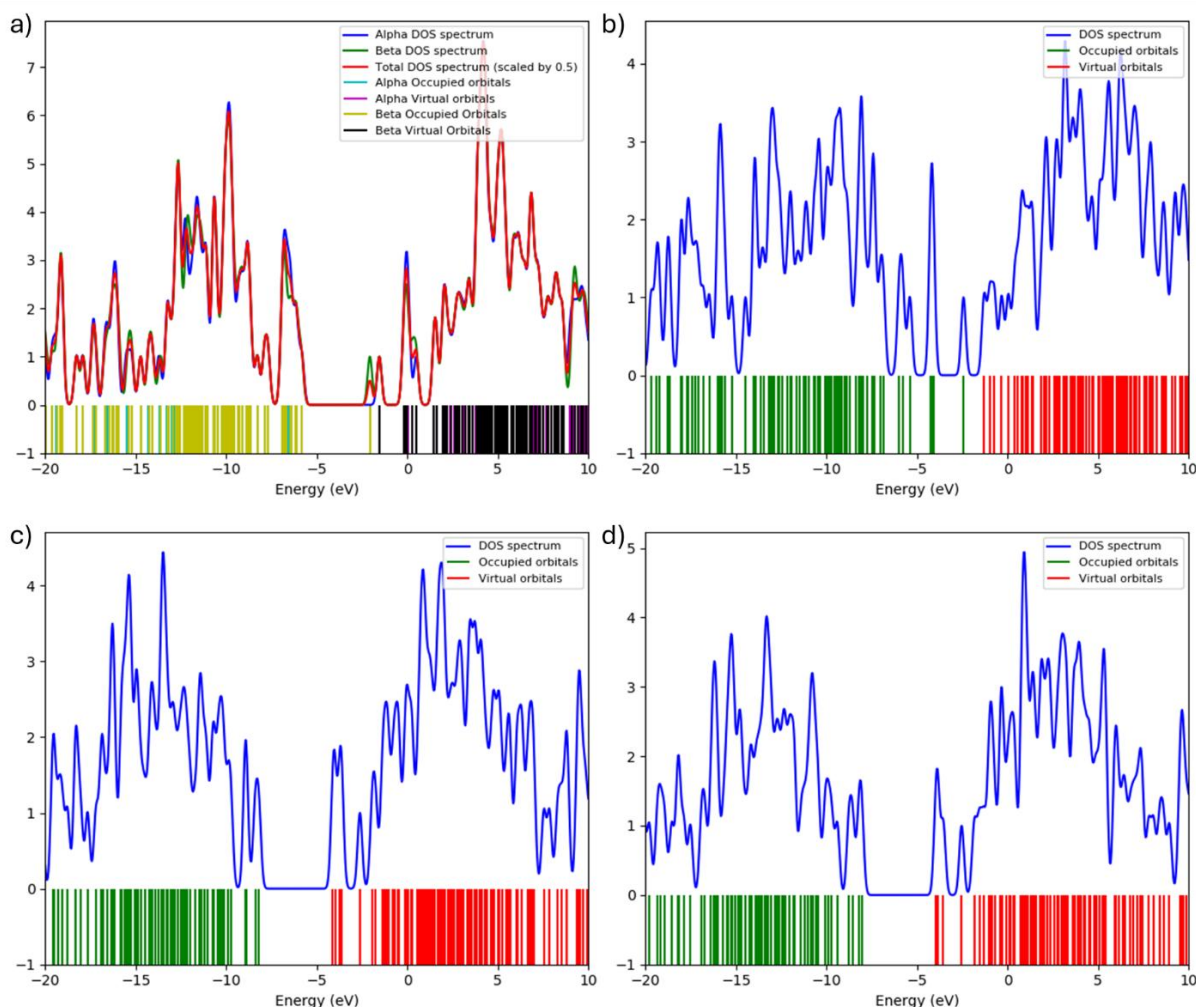


Figure 7. Density of states (DOS) of a) Ru-486-Ph, b) Ru-486-KOH, c) Ru-486-NO₂, d) Ru-486-OH molecules.

4. Discussion and Conclusion

This comprehensive study underscores the critical role of Mifepristone (RU-486) and its derivatives in breast cancer prevention and treatment. By employing advanced computational methods, including Density Functional Theory (DFT) and various spectroscopic techniques, we have successfully elucidated the structural and electronic properties of RU-486 and its derivatives (Ph, KOH, NO₂, OH). The findings reveal these modifications significantly influence molecular geometry, electronic distribution, and chemical reactivity, which are crucial for enhancing the therapeutic potential of these compounds. The study highlights the nucleophilic tendency of RU-486 derivatives, which plays a pivotal role in their interactions with biological targets. The promising antitumor activity of Mifepristone, especially when incorporated into nanosized drug delivery systems like liposomes and micelles, was confirmed. These systems demonstrated enhanced efficacy by effectively penetrating tumor tissues, inhibiting cancer-associated fibroblast (CAF) activation, reducing extracellular matrix (ECM) deposition, and decreasing tumor angiogenesis, leading to significant inhibition of breast cancer metastasis. Using computational tools such as DOS analysis, UV-Visible spectroscopy, NMR, and MEP mapping provided deep insights into the molecular dynamics and potential reactivity of RU-486 and its derivatives. These insights are invaluable for understanding the mechanisms of action and optimizing the design of new pharmaceutical compounds. This study reinforces the importance of combining computational chemistry with experimental validation to develop more effective chemo preventive and therapeutic strategies against breast cancer. The findings pave the way for future research and development of targeted therapies, contributing to better outcomes in breast cancer treatment.

Acknowledgements

This study is derived from a doctoral thesis conducted at the Institute of Science, Firat University. Mehmet Hanifi KEBİROĐLU was a doctoral student in the Computational Science and Engineering sub-department supported by the 100/2000 scholarship program of the Council of Higher Education (YÖK). The authors would like to thank his doctoral thesis advisor, Prof. Dr. Niyazi BULUT, for his valuable contributions.

References

- Aghdasi, P., Yousefi, S., & Ansari, R. (2024). Doping-induced changes in the structural and mechanical properties of germanene monolayers: A DFT-Based study. *Materials Science in Semiconductor Processing*, 174, 108246. <https://doi.org/10.1016/j.mssp.2024.108246>
- Aloumko, B., Foadin, C. S. T., Mohammadou, S., Nya, F. T., & Ejuh, G. W. (2024). Influence of metal oxides on circumcorannulene for the design of new push-pull corannulene models: applications in nano-electronics, optoelectronics and non-linear optics. *Molecular Simulation*, 50(5), 353–366. <https://doi.org/10.1080/08927022.2024.2316072>
- Araújo, C. F., Abranches, D. O., Coutinho, P., Vaz, P. D., Paulo Ribeiro-Claro, & Nolasco, M. M. (2024). Good vibrations: understanding deep eutectic solvents through the lens of vibrational spectroscopy. *Applied Spectroscopy Reviews*, 60(2), 137-192. <https://doi.org/10.1080/05704928.2024.2390962>
- Bartkowiak-Wieczorek, J., Jaros, A., Gajdzińska, A., Wojtyła-Buciora, P., Igor Szymański, Szymaniak, J., Janusz, W., Walczak, I., Jonaszka, G., & Bienert, A. (2024). The dual faces of oestrogen: the impact of exogenous oestrogen on the physiological and pathophysiological functions of tissues and organs. *International Journal of Molecular Sciences*, 25(15), 8167. <https://doi.org/10.3390/ijms25158167>
- Cao, Y., Balduf, T., Beachy, M. D., Bennett, M. C., Bochevarov, A. D., Chien, A., Dub, P. A., Dyall, K. G., Furness, J. W., Halls, M. D., Hughes, T. F., Jacobson, L. D., Kwak, H. S., Levine, D. S., Mainz, D. T., Moore, K. B., Svensson, M., Videla, P. E., Watson, M. A., & Friesner, R. A. (2024). Quantum chemical package jaguar: A survey of recent developments and unique features. *The Journal of Chemical Physics*, 161(5), 052502. <https://doi.org/10.1063/5.0213317>

- Chalbot, M.-C. G., & Kavouras, I. G. (2014). Nuclear magnetic resonance spectroscopy for determining the functional content of organic aerosols: A review. *Environmental Pollution*, *191*, 232–249. <https://doi.org/10.1016/j.envpol.2014.04.034>
- Chatterjee, S., Afzal, M., Mandal, P. C., Modak, R., Guin, M., & Konar, S. (2024). Exploration of supramolecular interactions, hirshfeld surface, FMO, molecular electrostatic potential (MEP) analyses of pyrazole based Zn(II) complex. *Journal of the Indian Chemical Society*, *101*(10), 101275. <https://doi.org/10.1016/j.jics.2024.101275>
- Chaudhuri, D., Majumder, S., Datta, J., & Giri, K. (2024). Elucidating the conformational change of dengue envelope protein using the Markov state model. *Molecular Simulation*, *50*(15), 1153–1169. <https://doi.org/10.1080/08927022.2024.2387126>
- Chen, Z., Long, L., Wang, J., Jiang, M., Li, W., Cui, W., & Zou, L. (2024). Enhanced tumor site accumulation and therapeutic efficacy of extracellular matrix-drug conjugates targeting tumor cells. *Small*, *20*, 2402040. <https://doi.org/10.1002/smll.202402040>
- Ciebiera, M., Kociuba, J., Ali, M., Madueke-Laveaux, O. S., Yang, Q., Bączkowska, M., Włodarczyk, M., Žeber-Lubecka, N., Zarychta, E., Corachán, A., Alkhrait, S., Somayeh, V., Malasevskaia, I., Łoziński, T., Laudański, P., Spaczynski, R., Jakiel, G., & Al-Hendy, A. (2024). Uterine fibroids: current research on novel drug targets and innovative therapeutic strategies. *Expert Opinion on Therapeutic Targets*, *28*(8), 669–687. <https://doi.org/10.1080/14728222.2024.2390094>
- Çankaya, N., Kebiroğlu, M. H., & Temüz, M. M. (2024). A comprehensive study of experimental and theoretical characterization and *in silico* toxicity analysis of new molecules. *Drug and Chemical Toxicology*, *47*(6), 1226–1240. <https://doi.org/10.1080/01480545.2024.2353724>
- Elia, A., Pataccini, G., Saldain, L., Ambrosio, L., Lanari, C., & Rojas, P. (2024). Antiprogestins for breast cancer treatment: We are almost ready. *The Journal of Steroid Biochemistry and Molecular Biology*, *241*, 106515. <https://doi.org/10.1016/j.jsbmb.2024.106515>
- Esselman, B. J., Zdanovskaia, M. A., Amberger, B. K., Shutter, J. D., Owen, A. N., Billingham, B. E., Zhao, J., Kisiel, Z., Woods, R. C., & McMahon, R. J. (2024). Millimeter-wave and high-resolution infrared spectroscopy of the low-lying vibrational states of pyridazine isotopologues. *The Journal of Chemical Physics*, *160*(19), 194301. <https://doi.org/10.1063/5.0205488>
- Ghazy, A. R., Abdel Gawad, S. A., Ghazy, R., El-Sharkawy, A. N., Hemeda, O. M., & Henaish, A. M. A. (2024). Structure, optical properties, TD-DFT simulations for nanosecond and continuous laser irradiation of vanadium antimony borate glass doped with nickel ferrite. *Scientific Reports*, *14*(1), 89. <https://doi.org/10.1038/s41598-023-50364-1>
- Günther, H. (2013). *NMR spectroscopy: basic principles, concepts, and applications in chemistry*. Wiley-Vch.
- He, X.-Y., Gao, Y., Ng, D., Michalopoulou, E., George, S., Adrover, J. M., Sun, L., Albrengues, J., Daßler-Plenker, J., Han, X., Wan, L., Wu, X. S., Shui, L. S., Huang, Y.-H., Liu, B., Su, C., Spector, D. L., Vakoc, C. R., Van Aelst, L., & Egeblad, M. (2024). Chronic stress increases metastasis via neutrophil-mediated changes to the microenvironment. *Cancer Cell*, *42*(3), 474–486.e12. <https://doi.org/10.1016/j.ccell.2024.01.013>
- Iftikhar, A., Shepherd, S., Jones, S., & Ellis, I. (2024). Effect of mifepristone on migration and proliferation of oral cancer cells. *International Journal of Molecular Sciences*, *25*(16), 8777. <https://doi.org/10.3390/ijms25168777>
- Irfan, A., Imran, M., Khalid, N., Ahmad, M., Chaudhry, A. R., Hussien, M., DaifAllah, S. Y., Al-Sehemi, A. G., Almalki, H. D., Qayyum, M. A., Saral, A., Manikandan, A., & Muthu, S. (2024). Molecular level interaction, HOMO-LUMO, MEP, UV-Vis, Hirshfeld, topological analysis, and in-vitro of isoflavones from *Eremostachys Vicaryi* Benth. Ex Hook. f. *Journal of Molecular Structure*, *1303*, 137581. <https://doi.org/10.1016/j.molstruc.2024.137581>
- Kebiroglu, M. H., & Ak, F. (2023). Molecular structure, geometry properties, Homo-Lumo, and mep analysis of acrylic acid based on DFT calculations. *Journal of Physical Chemistry and Functional Materials*, *6*(2), 92-100. <https://doi.org/10.54565/jphcfum.1343235>
- Kebiroglu, M. H., & Yilmaz, M. (2023). Investigation of UV-Visible absorption quantum effects doped of norepinephrine, Mg+2 atom by using DFT method. *Journal of Physical Chemistry and Functional Materials*, *6*(2), 145-151. <https://doi.org/10.54565/jphcfum.1332113>

- Kumar, A. R., Ilavarasan, L., Mol, G. P. S., Selvaraj, S., Azam, M., Jayaprakash, P., Kesavan, M., Alam, M., Dhanalakshmi, J., Al-Resayes, S. I., & Ravi, A. (2024). Spectroscopic (FT-IR, FT-Raman, UV-Vis and NMR) and computational (DFT, MESP, NBO, NCI, LOL, ELF, RDG and QTAIM) profiling of 5-chloro-2-hydroxy-3-methoxybenzaldehyde: A promising antitumor agent. *Journal of Molecular Structure*, 1298(1), 136974. <https://doi.org/10.1016/j.molstruc.2023.136974>
- Kundu, M., Butti, R., Panda, V. K., Malhotra, D., Das, S., Mitra, T., Prachi Kapse, Gosavi, S. W., & Kundu, G. C. (2024). Modulation of the tumor microenvironment and mechanism of immunotherapy-based drug resistance in breast cancer. *Molecular Cancer*, 23(1), 92. <https://doi.org/10.1186/s12943-024-01990-4>
- Liu, X., Liao, T., Yang, N., Ban, S., Wang, Y., Zheng, Z., & Zhou, Z. (2024). Synthesis, crystal and molecular structures, DFT calculations, spectroscopic (IR, NMR, UV-Vis), vibrational properties and Hirshfeld surface and antitumor activity of two pyrazole boronic acid pinacol ester compounds. *Journal of Molecular Structure*, 1299, 137204. <https://doi.org/10.1016/j.molstruc.2023.137204>
- Lv, Y., Li, W., Liao, W., Jiang, H., Liu, Y., Cao, J., Lu, W., & Feng, Y. (2024). Nano-drug delivery systems based on natural products. *International Journal of Nanomedicine*, 19, 541-569. <https://doi.org/10.2147/ijn.s443692>
- Manakkadan, V., Haribabu, J., Palakkeezhillam, V. N. V., Rasin, P., VEDIYAPPAN, R., Kumar, V. S., Garg, M., Bhuvanesh, N., & Sreekanth, A. (2024). Copper-mediated cyclization of thiosemicarbazones leading to 1,3,4-thiadiazoles: Structural elucidation, DFT calculations, in vitro biological evaluation and in silico evaluation studies. *Spectrochimica Acta Part a Molecular and Biomolecular Spectroscopy*, 313, 124117. <https://doi.org/10.1016/j.saa.2024.124117>
- Mello, S. L. A., Pereira, R. C., Codeço, C. F. S., Martinez, R., da Silveira, E. F., & Sant'Anna, M. M. (2024). Disorder analysis in infrared spectroscopy of acetylene ice. *The Journal of Physical Chemistry A*, 128(34), 7073-7083. <https://doi.org/10.1021/acs.jpca.4c02709>
- Middleton, J. R., Ghadiri, M., & Scott, A. J. (2024). Triboelectric charging properties of the functional groups of common pharmaceutical materials using density functional theory calculations. *Pharmaceutics*, 16(3), 433. <https://doi.org/10.3390/pharmaceutics16030433>
- Mohammad-Jafari, K., Naghib, S. M., & Mozafari, M. R. (2024). Cisplatin-based liposomal nanocarriers for drug delivery in lung cancer therapy: Recent progress and future outlooks. *Current Pharmaceutical Design*, 30(36), 2850-2881. <https://doi.org/10.2174/0113816128304923240704113319>
- Mustafa, M., Abbas, K., Alam, M., Ahmad, W., Moinuddin, N., Usmani, N., Siddiqui, S. A., & Habib, S. (2024). Molecular pathways and therapeutic targets linked to triple-negative breast cancer (TNBC). *Molecular and Cellular Biochemistry*, 479(4), 895-913. <https://doi.org/10.1007/s11010-023-04772-6>
- Naqvi, R., Ahmed, Z., Zameer, S., & Das, G. K. (2025). Drugs used in gynecology. *Ricos Biology*, 3(1), 122-148.
- Narwal, S., Vashist, M., Kaushik, R., Kalra, V., Hooda, R., & Singh, S. (2024). *A systematic review on uterine leiomyoma: From pathogenomics to therapeutics*. IntechOpen eBooks. <https://doi.org/10.5772/intechopen.1002877>
- Obeagu, E. I., & Obeagu, G. U. (2024). Breast cancer: A review of risk factors and diagnosis. *Medicine*, 103(3), e36905. <https://doi.org/10.1097/md.00000000000036905>
- Pracht, P., Grimme, S., Bannwarth, C., Bohle, F., Ehlert, S., Feldmann, G., Gorges, J., Müller, M., Neudecker, T., Plett, C., Spicher, S., Steinbach, P., Wesolowski, P. A., & Zeller, F. (2024). CREST—A program for the exploration of low-energy molecular chemical space. *The Journal of Chemical Physics*, 160(11), 114110. <https://doi.org/10.1063/5.0197592>
- Rahuman, M. H., Muthu, S., Raajaraman, B. R., Raja, M., & Umamahesvari, H. (2020). Investigations on 2-(4-Cyanophenylamino) acetic acid by FT-IR, FT-Raman, NMR and UV-Vis spectroscopy, DFT (NBO, HOMO-LUMO, MEP and Fukui function) and molecular docking studies. *Heliyon*, 6(9), e04976. <https://doi.org/10.1016/j.heliyon.2020.e04976>
- Rajimon, K. J., Alzahrani, A. Y., Aazam, E. S., Abbas, B. M., Govindarajan, P., & Thomas, R. (2024). Unveiling the multifaceted potential of (E)-N-(4-Chlorophenyl)-1-(thiophen-2-yl) methanimine

- with special reference to solution-state fluorescence, synthesis, electronic structure, antimicrobial, antibiofilm, larvicidal activities, toxicity, docking and dynamics. *Journal of Molecular Structure*, 1302, 137428. <https://doi.org/10.1016/j.molstruc.2023.137428>
- Sayed, Z. S., Khattap, M. G., Madkour, M. A., Yasen, N. S., Elbary, H. A., Elsayed, R. A., Abdelkawy, D. A., Wadan, A. S., Omar, I., & Nafady, M. H. (2024). Circulating tumor cells clusters and their role in breast cancer metastasis; a review of literature. *Discover Oncology*, 15(1), 94. <https://doi.org/10.1007/s12672-024-00949-7>
- Seqqat, Y., El Monfalouti, H., Anouar, E. H., Laaraj, S., Mague, J. T., Chahdi, F. O., Rodi, Y. K., Essassi, E. M., & Sebbar, N. K. (2025). Experimental and theoretical investigations for novel 6-nitroquinoxaline-2,3-dione derivatives: Synthesis, characterization, DFT calculations, ADME analysis, hirshfeld surface calculations, molecular docking studies, and antiproliferation evaluation. *Journal of Molecular Structure*, 1319, 139612. <https://doi.org/10.1016/j.molstruc.2024.139612>
- Şahin, S. (2023). A new molecular structure and computational analyses: DFT studies, NLO properties, ADMET predictions, biological targets, and docking experiments. *Polycyclic Aromatic Compounds*, 44(6), 4029-4043. <https://doi.org/10.1080/10406638.2023.2244630>
- Tegegn, D. F., Belachew, H. Z., & Salau, A. O. (2024). DFT/TDDFT calculations of geometry optimization, electronic structure and spectral properties of clevidine and telbivudine for treatment of chronic hepatitis B. *Scientific Reports*, 14(1), 8146. <https://doi.org/10.1038/s41598-024-58599-2>
- Utjés, D., Boggavarapu, N. R., Rasul, M. F., Koberg, I., Zulliger, A., Ponandai-Srinivasan, S., Von Grothusen, C., Lalitkumar, P. G., Papaikononou, K., Alkasalias, T., & Gemzell-Danielsson, K. (2024). Transcriptomic profile of breast tissue of premenopausal women following treatment with progesterone receptor modulator: Secondary outcomes of a randomized controlled trial. *International Journal of Molecular Sciences*, 25(14), 7590. <https://doi.org/10.3390/ijms25147590>
- Wu, J., Lu, Q., Zhao, J., Ding, H., Zhu, L., Wang, Z., Wu, W., Sun, S., Wang, Q., & Zhang, B. (2024). Mixtures of doxorubicin-loaded micelles and berberine and mifepristone co-loaded liposomes inhibit breast cancer metastasis based on regulation of tumor microenvironments. *ACS Applied Nano Materials*, 7(9), 10748-10759. <https://doi.org/10.1021/acsanm.4c01269>
- Xiong, X., Zheng, L. W., Ding, Y., Chen, Y. F., Cai, Y. W., Wang, L. P., Huang, L., Liu, C. C., Shao, A. M., & Yu, K. D. (2025). Breast cancer: pathogenesis and treatments. *Signal Transduction and Targeted Therapy*, 10(1), 49. <https://doi.org/10.1038/s41392-024-02108-4>
- Xue, R., Pan, Y., Xia, L., & Li, J. (2024). Non-viral vectors combined delivery of siRNA and anti-cancer drugs to reverse tumor multidrug resistance. *Biomedicine & Pharmacotherapy*, 178, 117119. <https://doi.org/10.1016/j.biopha.2024.117119>
- Yılmaz, M., & Kebiroglu, M. H. (2024). Nuclear magnetic resonance and quantum chemical calculations of Ca²⁺ doped norepinephrine molecule by using DFT and HF methods. *International Journal of Pure and Applied Sciences*, 10(1), 1-11. <https://doi.org/10.29132/ijpas.1376725>
- Zaki, K., Ouabane, M., Sbai, A., Sekkate, C., Bouachrine, M., & Lakhlifi, T. (2025). Unraveling the mechanism, regioselectivity, and stereoselectivity of [3+ 2] cycloaddition reactions for anticancer spirooxindole derivatives: A density functional theory study. *Computational and Theoretical Chemistry*, 1245, 115086. <https://doi.org/10.1016/j.comptc.2025.115086>
- Zhang, N., Zhou, J., Li, S., Cai, W., Ru, B., Hu, J., Liu, W., Liu, X., Tong, X., & Zheng, X. (2024a). Advances in nanoplateforms for immunotherapy applications targeting the tumor microenvironment. *Molecular Pharmaceutics*, 21(2), 410-426. <https://doi.org/10.1021/acs.molpharmaceut.3c00846>
- Zhang, J., Li, J., Wang, Y., & Shi, C. (2024b). NMR methods to detect fluoride binding and transport by membrane proteins. *Methods in Enzymology*, 696, 25-42. <https://doi.org/10.1016/bs.mie.2023.12.009>
- Zheng, J., & Hao, H. (2024). The importance of cancer-associated fibroblasts in targeted therapies and drug resistance in breast cancer. *Frontiers in Oncology*, 13. <https://doi.org/10.3389/fonc.2023.1333839>